Cubic Group 13 Heterosiloxanes with Four $Co_3(CO)_9C$ Cluster Units as Substituents: Novel Soluble Model Compounds for Synthetic Zeolites Showing Catalytic Activity in Hydroformylation Reactions

Uwe Ritter, Norbert Winkhofer, Ramaswamy Murugavel, Andreas Voigt, Dietmar Stalke, and Herbert W. Roesky*

Contribution from the Institute of Inorganic Chemistry, University of Göttingen, Tammannstrasse 4, D-37077 Göttingen, Germany

Received August 30, 1995[⊗]

Abstract: The reactions between the cobalt carbonyl anchored silanetriol $Co_3(CO)_9CSi(OH)_3$ (**1**) and EMe_3 (E = Al, Ga and In) in THF result in the formation of the respective group 13 heterosiloxanes $[Co_3(CO)_9CSiO_3E{\cdot}THF]_4$ (Al (**2**); Ga (**3**); In (**4**)) in good yields. The new heterosiloxanes have been extensively characterized by means of their analytical and spectroscopic (mass, IR, and NMR) data. Additionally, the molecular structure of the Al complex **2** has been determined by X-ray diffraction studies. The compound contains a cubic $Al_4O_{12}Si_4$ core with four $Co_3(CO)_9C$ cluster units anchored on each of the silicon atoms at the alternating corners of the cube. Interestingly, there are three different types of $Co_3(CO)_9C$ cluster units within the same molecule based on the mode of coordination of the CO ligands. In order to test the utility of these compounds in catalytic conversions, hydroformylation reactions involving 1-hexene as substrate have been carried out at 120 °C under a H_2/CO initial pressure of 70 bar. A series of solution studies of the catalytic mixture (such as time-dependent IR, NMR, and MS) have been carried out in order to identify the catalytic active species in the process. The Al- and Ga-containing heterosiloxanes show a better hydroformylation activity compared to the In analogue. The regioselectivity of the hydroformylation reactions with **2** is found to be over 60%. The hydroformylation presumably proceeds via the decomposition of $Co_3(CO)_9C$ cluster fragments into $Co_2(CO)_8$ units in the case of catalysts **2** and **3**.

Introduction

The hydroformylation of terminal olefins is a well-known industrial process for the large-scale preparation of aldehydes involving homogeneous catalytic systems (eq 1). At high

$$RCH{=}CH_2 + CO + H_2 \xrightarrow{\text{catalyst}} RCH_2CH_2CHO + \underset{\displaystyle CH_3}{\overset{\displaystyle |}{RCHCHO}} \qquad (1)$$

temperatures and pressures, hydroformylation reactions have been found to be catalyzed by group 9 carbonyl clusters, of which cobalt based clusters have been extensively studied.[1] The classical Roelen process employed cobalt metal as the catalyst and the catalytically active species in this homogeneous process was believed to be $HCo(CO)_4$.[2] However, the major disadvantage in using this reaction process is the remarkably high volatility of the catalyst. This led to a search for rather more expensive rhodium-based catalysts for this purpose.[3]

Anchoring active catalysts to insoluble materials such as oxides, silicates, and zeolites cuts the loss of catalyst during the catalytic process.[4−7] The fixation of the active centers can be achieved either by means of their interaction with the hydroxyl groups on a solid surface or alternatively by means of interactions between the CO ligands and a Lewis acidic center of the surface. Similar cobalt-doped zeolites as catalysts for hydroformylation reactions have been reported.[8] In those cases the metal species have been deposited in the form of salts or carbonyl clusters. Furthermore, the modifications of oxidic surfaces with the multinuclear cobalt carbonyl cluster $Co_3(CO)_9CR$ (R = CH_3;[9] Ph[10]) have been reported.

Our interest in this area is centered around synthesizing soluble cluster compounds that mimic surface catalysts. Feher et al. have contributed to this idea by their work on metallasilasesquioxanes.[11−13] Additionally Calzaferri et al. reported the synthesis of the cubic spherosilicate $Co(CO)_4(H_7Si_8O_{12})$, which is interesting with regard to mimicing surface-fixed cobalt clusters[14] although no studies on the catalytic activity of this compound have been described.

We have recently initiated a research program on devising synthetic routes for a variety of silanetriols of the formula $RSi(OH)_3$ (where R is an alkyl, amino, or aryloxy group) in order

[⊗] Abstract published in *Advance ACS Abstracts,* August 15, 1996.

(1) Gladfelter, W. L.; Roesselet, K. J. *The Chemistry of metal cluster complexes*; Shriver, D. F., Kaesz, H. D., Adams, R. D., Eds.; VCH: New York, 1990; pp 344−346.

(2) There have been several mechanistic studies to identify the real active species in this system.

(3) Cornils, B.; Herrmann, W. A.; Rasch, M. *Angew. Chem., Int. Ed. Engl.* **1994**, *33*, 2144.

(4) *Studies in Surface Science and Catalysis 29: Metall Clusters in Catalysis*; Gates, B. C., Guczi, L., Knözinger, H., Eds.; Elsevier: Amsterdam, Oxford, New York, Tokyo, 1986.

(5) *Studies in Surface Science and Catalysis 5: Catalysis by Zeolites*; Elsevier: Amsterdam, Oxford, New York, Tokyo, 1980.

(6) Gates, B. C. *Angew. Chem., Int. Ed. Engl.* **1993**, *32*, 228.

(7) Ichikawa, M.; Rao, L.-f.; Fukuoka, A. *Catalytic Science and Technology*; Yoshida, S., Takezawa, N., Ono, T., Eds.; VCH: Weinheim; Kodansha: Tokyo, 1991; Vol. 1, pp 111−116.

(8) Maxwell, E. *Advances in Catalysis 31*; Eley, D. D., Pines, H., Weisz, P. B., Eds.; Academic Press: New York, 1982.

(9) Schneider, R. L.; Howe, R. F.; Watters, K. L. *J. Catal.* **1983**, *79*, 298.

(10) Meyers, G. F.; Hall, M. B. *Organometallics* **1985**, *4*, 1770.

(11) Feher, F. J.; Budzichowski, T. A.; Weller, K. J. *J. Am. Chem. Soc.* **1989**, *111*, 7288.

(12) Feher, F. J.; Weller, K. J. *Organometallics* **1990**, *9*, 2638.

(13) Feher, F. J.; Budzichowski, T. A. *Polyhedron* **1995**, *14*, 3239.

(14) Calzaferri, G.; Imhoff, R.; Törnroos, K. W. *J. Chem. Soc., Dalton Trans.* **1993**, 3741.

S0002-7863(95)02986-6 CCC: $12.00

Scheme 1

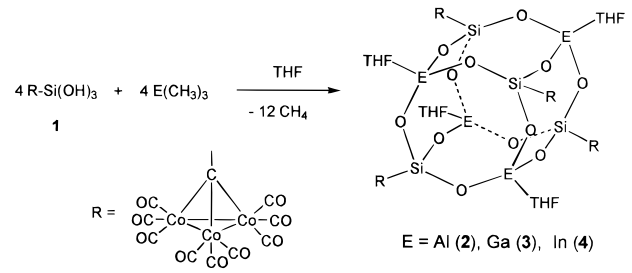

to use them for supporting catalytically active metal centers. Subsequently we were able to interact these silanetriols with a variety of metal substrates and prepare a multitude of metallasiloxanes.[15] For example, the interaction of solid Re_2O_7 with *t*-BuSi(OH)$_3$ results in the formation of an eight-membered siloxane ring on which four ReO_4 fragments are anchored.[16] Likewise the first molecular alumino- and gallasiloxanes synthesized by us[17−19] and others[20,21] can be considered as the smaller analogues of synthetic zeolites.

Therefore, it was our purpose to extend these investigations in the lines of realizing such useful species with group 9 carbonyl clusters anchored on them. Accordingly, we chose to synthesize the cobalt carbonyl based silanetriol $Co_3(CO)_9CSi(OH)_3$ (**1**),[22] originally reported by Seyferth,[23] and react it with group 13 alkyls such as $AlMe_3$. The results of this investigation along with their use as hydroformylation catalysts are reported in this paper.

Results and Discussion

Synthesis and Spectra. The reactions between tricobalt nonacarbonyl methylidyne silanetriol **1** and equimolar quantities of group 13 trimethyl derivatives in THF leads to the isolation of the Al-, Ga-, and In-containing heterosiloxanes **2**−**4** in good yields (Scheme 1). The reaction is complete within a few minutes in each case as monitored by the evolution of methane gas. However, in the case of Ga and In, the reaction mixture was further heated under reflux to ensure the completion of the reaction.

The products were isolated in an analytically pure form and characterized by elemental analysis and mass, IR, and NMR (^{1}H, ^{13}C, and ^{29}Si) spectroscopic measurements. All the compounds yielded satisfactory analytical data. However, we were not able to either observe the molecular ion peaks in their mass spectra or obtain melting points. On heating above 200 °C, a considerable amount of decomposition is observed. The solubility of these compounds in hexane increases in the order **4** > **3** > **2**. However, all the compounds are highly soluble in polar solvents such as THF.

The CO region of the IR spectra of **2** and **3** along with the spectrum of $Co_2(CO)_8$ (for comparison purposes) is shown in Figure 1.[24] All the compounds show a very similar spectral pattern in this region showing two strong absorptions between 2000 and 2100 cm^{-1}.

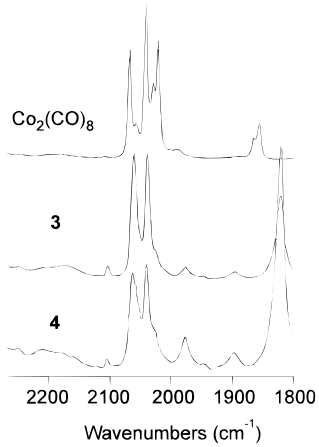

Figure 1. FTIR spectra of **4**, **3**, and $Co_2(CO)_8$ in hexane solution at 20 °C before catalytic runs. Peak at 1821 cm^{-1} are due to 1-hexene.

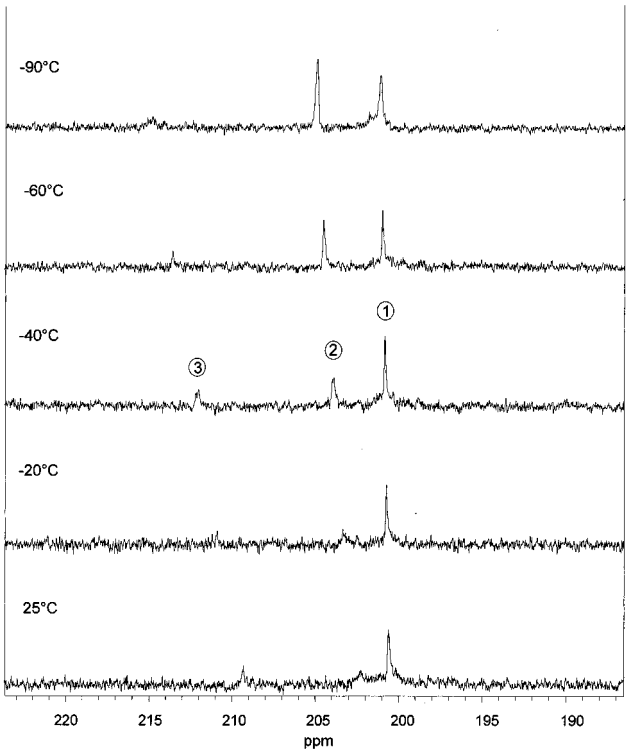

Figure 2. Variable-temperature ^{13}C NMR spectra of the CO region of cluster **3** in THF-d_8.

The ^{13}C NMR temperature dependent solution studies in the region of carbonyl carbon nuclei show dynamic behavior. Variable-temperature experiments for compounds **3** and **4** were performed between 20 and −90 °C in THF-d_8 and the results are summarized in Figures 2 and 3, respectively. It is generally observed that there is a fast intramolecular exchange process between the axial and equatorial CO ligands even at temperatures as low as −90 °C in the case of complexes of the type $Co_3(CO)_9CR$.[25] Thus, there is only one signal observed for all the CO ligands in these compounds. In the present study, the Ga heterosiloxane **3** shows the presence of three signals even at 25 °C (Figure 2). On cooling, there does exist some change

(15) Murugavel, R.; Chandrasekhar, V.; Roesky, H. W. *Acc. Chem. Res.* **1996**, *29*, 183.
(16) Winkhofer, N.; Roesky, H. W.; Noltemeyer, M.; Robinson, W. T. *Angew. Chem., Int. Ed. Engl.* **1992**, *31*, 599.
(17) Montero, M. L.; Usón, I.; Roesky, H. W. *Angew. Chem., Int. Ed. Engl.* **1994**, *33*, 2103.
(18) Voigt, A.; Murugavel, R.; Parsini, E.; Roesky, H. W. *Angew. Chem., Int. Ed. Engl.* **1996**, *35*, 748.
(19) Voigt, A.; Murugavel, R.; Parsini, E.; Roesky, H. W. In preparation.
(20) Hoebbel, D.; Garzó, G.; Ujszászi, K.; Engelhardt, G.; Fahlke, B.; Vargha, A. *Z. Anorg. Allg. Chem.* **1982**, *484*, 7.
(21) Smolin, Yu. I.; Shepelev, Yu. F.; Ershov, A. S.; Khobbel, D. *Dokl. Akad. Nauk SSSR* **1987**, *297*, 1377; *Chem. Abstr.* **1988**, *108*, 229950 f.
(22) Ritter, U.; Winkhofer, N.; Schmidt, H.-G.; Roesky, H. W. *Angew. Chem., Int. Ed. Engl.* **1996**, *35*, 524.
(23) Seyferth, D.; Nivert Rudie, C.; Ozolins Nestle, M. *J. Organomet. Chem.* **1979**, *178*, 227.

(24) Due to the poor solubility of the Al compound **2** in *n*-hexane, a solution spectrum for this compound could not be obtained. The spectrum was recorded only as a Nujol mull.

Table 1. Summary of the Hydroformylation Studies

expt no.[a]	catalyst	catalyst concn, mmol	1-hexene conversion, %[b]	% of 1-hexene converted in to aldehydes[c]	internal olefins, mmol (%)[d]	1-heptanal, mmol	internal aldehydes, mmol	selectivity linear/ branched[e]	material balance, %[f]	turnover no. (18 h)[g]
1	**2**	0.02	83.8	95	6 (4)	90	44	2.0	89	6700
2	**2**	0.03	86.9	96	5 (3)	92	47	2.0	91	4633
3	**2**	0.04	91.3	98	3 (1)	98	48	2.0	93	3650
4	**3**	0.02	83.1	89	12 (8)	81	52	1.6	93	6650
5	**3**	0.03	87.5	91	11 (7)	86	54	1.6	96	4667
6	**3**	0.04	88.1	94	8 (5)	82	59	1.4	94	3525
7	**4**	0.025	13.1	15	24 (17)	12	9	1.3	89	840
8	**4**	0.03	21.9	25	38 (27)	19	16	1.2	88	1167
9	**4**	0.035	46.0	52	55 (37)	34	42,5	0.8	92	2186
10	**4**	0.04	58.8	62	56 (37)	35	59	0.6	94	2350

[a] Conditions: reaction time 18 h; reaction temperature 120 °C, initial pressure 70 bar; 1-hexene charged 160 mmol; toluene charged 30 mL; internal standard 5 mL heptane. [b] Percent conversion − mmol of aldehyde/mmol of 1-hexene charged. [c] Percent of unrecovered 1-hexene converted to aldehydes; loss of hexene occurs during charging and depressurization of the autoclave. [d] Internal olefin = 2-hexene and 3-hexene; used 1-hexene contains 3% internal olefins. [e] Selectivity linear/branched of the aldehydes. [f] The material balance is not 100% due to the loss of hexene. GC analysis at different high-temperature programs showed no high molecular weight products and only trace amounts of hydrogen products like hexane, heptanol, or 2-methylhexanol. [g] Turnover number: mmol of aldehydes/mmol of catalyst.

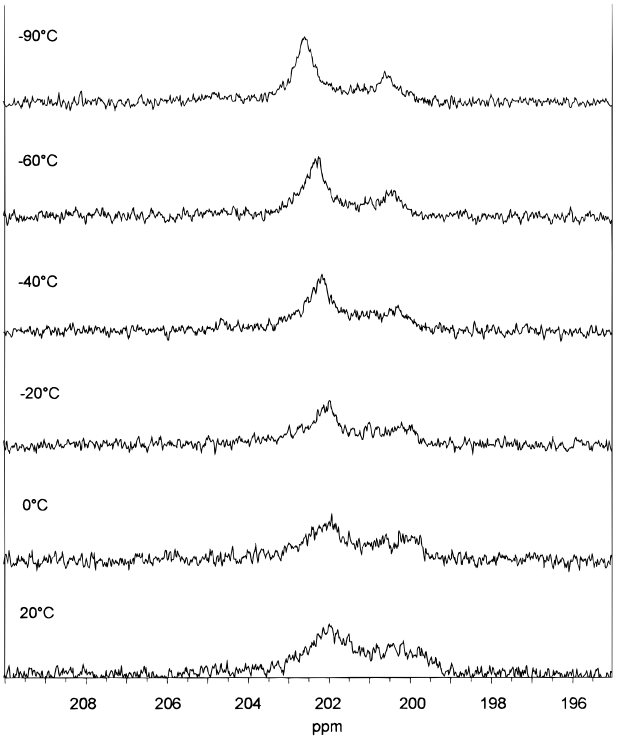

Figure 3. Variable-temperature ^{13}C NMR spectra of the CO region of cluster **4** in THF-d_8.

in the relative intensity of these lines, with the overall spectral pattern remaining the same. Although there is no straightforward assignment for these three peaks, from the crystal structure of the Al heterosiloxane **2** reported *vide infra*, we are tempted to assign these peaks to be originating from the (1) terminal, (2) bridging, and (3) semibridging type of CO ligands. As indicated previously by other authors,[25] the intramolecular exchange process in the present case also is very fast at room temperature and hence the intensity of the peak due to the bridging type of CO ligands is low. However, on cooling the solution to −90 °C, we observe the intensity of peak 2 to increase (Figure 2), possibly indicating that the number of $Co_3(CO)_9C$ units containing bridging CO ligands has increased. Another interesting observation in the ^{13}C NMR temperature-dependent spectra of compound **3** is the frequency shift of peaks 2 and 3. For example, peak 3 is downfield shifted by 5.5 ppm on cooling the solution to −90 °C from room temperature. Such behavior has been observed for phosphine-substituted $Co_3(CO)_8(PPh_3)CCH_3$ and this observation has been attributed to an increased lifetime of a phosphine ligand on a particular cobalt atom at lower temperature.[26] However, since complexes **2**−**4** do not have phosphine ligands and still show a similar behavior, we believe that this observation should have a relation to the increased number of bridging CO species at lower temperatures. On the other hand, the temperature-dependent spectra of the In analogue **4** is quite different. Firstly, only two very broad overlapping signals are observed in the CO region at room temperature as shown in Figure 3. Secondly, neither does this pattern change as a function of temperature nor there is any distinct sharpening of the lines. This is a clear indication of a very fast intramolecular CO exchange process in this case irrespective of the temperature of the spectral measurement. This observation is fully supported by $^{12}CO/^{13}CO$ exchange studies by mass spectroscopy discussed *vide infra*.

The ^{29}Si NMR spectra of these compounds show only one peak which is upfield shifted from the value of the parent silanetriol **1**, indicating that these compounds contain only one type of silicon in solution. While the resonance for **2** is observed at −73.6 ppm, the corresponding values for compounds **3** and **4** are downfield shifted and are observed at −63.6 and −62.5 ppm, respectively. This observation is consistent with the values observed for the group 13 heterosiloxanes derived from a series of aminosilanetriols.[27]

Molecular Structure of 2. Suitable single crystals of compound **2** can be obtained from the reaction mixture by adding hexane and storing the mixture under low temperature for prolonged periods. Compound **2** crystallizes in the monoclinic space group $P2_1/c$.[28−30] The molecular structure of **2** in the solid state with the atom labeling scheme is shown in Figure 4. Selected structural parameters are listed in Table 2. The Al/O/Si central core of the molecule contains a $Al_4O_{12}Si_4$ cubic framework whose alternating corners are occupied by aluminum and silicon atoms (Figure 5). Each of the cube edges are bridged by a μ^2-oxygen atom. Furthermore the four silicon atoms bind to cobalt methylidyne cluster $Co_3(CO)_9C$ units while each of the four aluminum atoms coordinate to a THF donor ligand.

(25) Aime, S.; Milone, L.; Valle, M. *Inorg. Chim. Acta* **1976**, *18*, 9.

(26) Matheson, T. W.; Robinson, B. H. *J. Organomet. Chem.* **1975**, *88*, 367.

(27) Voigt, A.; Murugavel, R.; Ritter, U.; Roesky, H. W. *J. Organomet. Chem.* In press.

(28) Kottke, T.; Stalke, D. *J. Appl. Crystallogr.* **1993**, *26*, 615.

(29) Sheldrick, G. M. *Acta Crystallogr. Sect. A* **1990**, *46*, 467.

(30) Sheldrick, G. M. Program SHELXL-93, University of Göttingen, 1993.

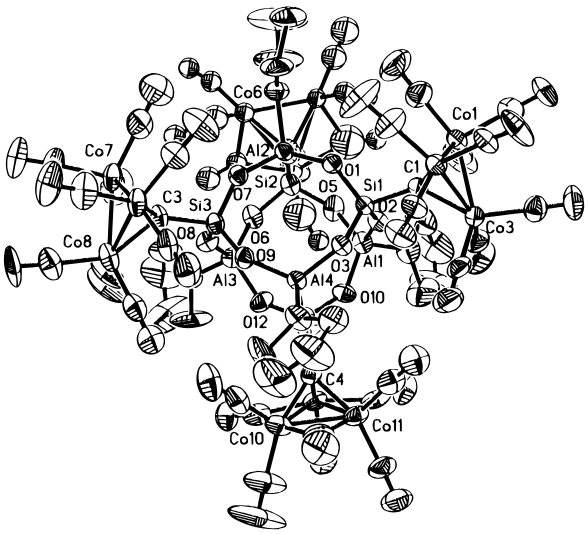

Figure 4. Solid-state structure of **2**.

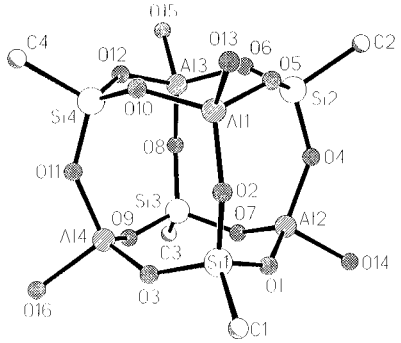

Figure 5. Solid-state structure of the aluminosiloxane core of **2** without Co substituents.

Table 2. Selected Bond Lengths (pm) and Angles (deg) for **2**

Co(1)−Co(3)	247.0(1)	Co(2)−Co(3)	246.6(1)
Co(1)−C(1)	190.0(6)	C(1)−Si(1)	185.5(6)
Co(2)−C(1)	189.8(6)	Si(1)−O(1a)	162.0(6)
Co(1)−Co(2)	247.5(1)	Si(1)−O(1b)	162.4(6)
Co(3)−C(1)	191.1(6)	Si(1)−O(1c)	164.4(6)
Co(3)−Co(1)−CO(2)	59.83(4)	Si(1)−C(1)−Co(3)	128.8(4)
C(1)−Co(2)−Co(3)	49.9(2)	O(1a)−Si(1)−O(1b)	111.2(4)
Co(3)−Co(2)−Co(1)	59.99(4)	Co(1)−C(1)−Co(3)	80.8(2)
C(1)−Co(2)−Co(1)	49.4(2)	O(1b)−Si(1)−O(1c)	105.9(3)
Co(2)−Co(3)−Co(1)	60.18(4)	O(1a)−Si(1)−O(1c)	106.4(3)
C(1)−Co(3)−Co(2)	49.4(2)	O(1b)−Si(1)−C(1)	110.2(3)
Si(1)−C(1)−Co(2)	128.8(4)	O(1a)−Si(1)−C(1)	110.8(3)
C(1)−Co(3)−Co(1)	49.4(2)	C(1)−Co(1)−Co(3)	49.8(2)
Co(2)−C(1)−Co(1)	81.3(2)	O(1c)−Si(1)−C(1)	112.2(3)
Si(1)−C(1)−Co(1)	136.4(4)	C(1)−Co(1)−Co(2)	49.3(2)
Co(2)−C(1)−Co(3)	80.7(2)		

This Al/O/Si framework of the molecule resembles the smallest three-dimensional unit (secondary building unit, SBU) of a zeolite[31] which has been found in the Linde Type A species.[32] The alternating arrangement of silicon, oxygen, and aluminum as well as the stoichiometry of the two metallic elements obey the Loewenstein rule or the so-called aluminum avoidance rule.[33] The silicon atoms are tetrahedrally surrounded by three oxygen atoms and the apical carbon atom of the cobalt methylidyne cluster. The Si−O bond lengths are in the range of 160.3(6) to 162.3(6) pm being relatively short compared to

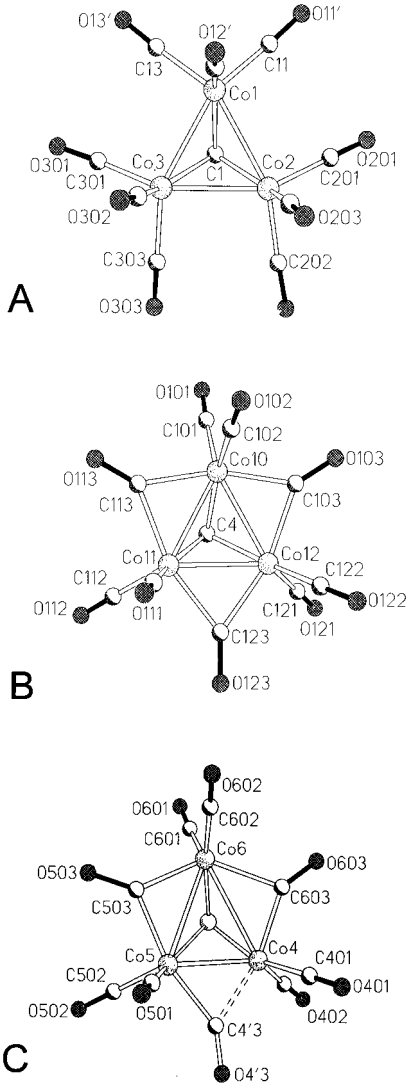

Figure 6. The three types of $Co_3(CO)_9C$ cluster fragments of **2** in the solid-state structure.

the corresponding bonds in $\{[(CH_3)_4N]_4^{4+}[Al_4O_{12}Si_4(OH)_8]^{4-}\}$.[21] They agree well with the average value (160.8 pm) given by Brown for Si−O distances in a silicate lattice.[34] The aluminum atoms are likewise tetrahedrally surrounded by four oxygen atoms. The Al−O bond lengths of the cubic core lie in the range 168.8(6) to 173.2(6) pm, which corresponds to an average bond length of 170.7 pm. This is in good agreement with the corresponding bond lengths found in $\{[(CH_3)_4N]_4^{4+}[Si_4O_{12}Al_4(OH)_8]^{4-}\}$ (170.0 pm).[21] However, the Si−O bond lengths are shorter than the corresponding calculated value (172.8 pm) for sodalite.[35] The Al−O bond lengths of the coordinated THF molecules (Figure 1) (184.4(6) to 186.0(7) pm) are significantly longer than those of the core Al−O distances.

The most interesting feature of the molecular structure of **2** is the geometry of the four surrounded tricobalt methylidyne nonacarbonyl units on silicon. These four carbonyl clusters have three distinctly different arrangements (**A**, **B**, and **C**) based on the binding mode of the CO ligands as depicted in Figure 6. This kind of arrangement is the first experimental observation for cobalt carbonyl clusters of the type $Co_3(CO)_9C$. The average Si−C distance (185.8 pm) is 5.4 pm shorter than the corresponding value found in compound **1**.[22]

(31) Gramlich-Meier, R.; Meier, W. M. *J. Solid State Chem.* **1982**, *44*, 41.
(32) Smith, J. V. *Chem. Rev.* **1988**, *88*, 149.
(33) Loewenstein, W. *Am. Mineral.* **1954**, *39*, 92.
(34) Brown, G. E.; Gibbs, G. V. *Am. Mineral.* **1969**, *54*, 1528.
(35) Wells, A. F. *Structural Inorganic Chemistry*, 4th ed.; Clarendon Press: Oxford 1975.

In all types, the three cobalt atoms form the corners of a triangle capped by a carbon atom. In type **A**, all of the nine CO ligands are terminally bonded and have an average metal−metal distance of 246.8 pm. This compares well with those in **1** (245.46(14)−247.58(12) pm). This type of terminally bonded CO ligand is exclusively found in the two clusters bonded to Si1 and Si3 of the molecule. In type **B**, which is bonded to Si4, three of the nine CO ligands are arranged in a bridging mode. The average metal−metal distance is 245.1 pm. While the Co_3 triangle in **A** and **B** is highly symmetric, this unit in cluster **C** is highly distorted. Here, six of the nine CO ligands are terminally bonded as in the case of type **B**. Two other CO ligands are present in a μ^2-bridged position and the remaining CO ligand (C4′3, Figure 6) is surprisingly semibridged (Co−C bond distance 191.7 pm). This semibridging ligand shows a weak interaction with the adjacent Co4 (Co−C bond distance, 198.2 pm).

The late transition metals with higher atomic numbers show an increasing tendency to form μ^2-bridged carbonyl clusters. This is attributed to the larger atomic radii resulting in reduced electron density in these atoms. The occurrence of bridging ligands in **2** indicates an electron-withdrawing effect of the aluminosiloxane framework on the cobalt methylidyne units. The electron-withdrawing nature of the cubic Si_8O_{12} siloxane framework has recently been experimentally demonstrated by Feher and co-workers for a series of spherosilicates.[36] Hence, it might be expected that the $E_4O_{12}Si_4$ (E = Al, Ga, In) frameworks in the heterosiloxanes **2**−**4** would also have similar electron-withdrawing effects on the $Co_3(CO)_9C$ substituents, resulting in bridging and semibridging CO ligands.

Hydroformylation Studies. The parent silanetriol **1** and the new heterosiloxanes **2**−**4** show catalytic activity in hydroformylation reactions involving 1-hexene. The use of **1** and related polyethylene glycol ethers of **1** for this purpose has already been described in a preliminary communication.[22] The summary of the present hydroformylation investigations using 1-hexene as the substrate is presented in Table 1. The experiments were performed at an initial CO/H_2 pressure of 70−80 bar. It should be noted that this pressure is significantly lower compared to the pressure of about 200 bar at which hydroformylation reactions with $Co_2(CO)_8$ are usually performed.[37]

As can be seen from Table 1, the Al and Ga catalysts **2** and **3** show a better catalytic activity than the In analogue **4**. For example, at a 0.02 mmol concentration of the catalysts **2** and **3**, the observed turnover numbers are 6700 and 6650, respectively. The corresponding value for In catalyst **4** after 18 h of the catalytic run is only 840. It is also interesting to note that the numbers observed for **2** and **3** are close to those observed for silanetriol **1**.

The significant observation in all these catalytic runs is the amount of 1-hexene converted into the aldehydes. While values closer to 90% are observed irrespective of the concentration of the catalysts for compounds **2** and **3**, in the case of In catalyst **4** this value is considerably lowered (Table 1). However, in the case of In catalyst **4**, a large amount of olefin isomerization is found to take place. This implies that the isomerization and hydroformylation reactions are taking place simultaneously. The former process results in the formation of internal olefins which are ultimately converted into aldehydes in the case of **2** and **3**. However, the hydroformylation process of the internal olefins is apparently less effective with In catalyst **4**. This leads to the isolation of substantial amounts of internal olefins at the end of catalytic runs (17−37% after 18 h). In order to test this supposition, we performed hydroformylation of 2-hexene under similar conditions with **4** and found little or no conversion of the olefin to aldehyde. Hence the results indicate that **2** and **3** are equally efficient for the hydroformylation of both terminal and branched olefins. On the other hand, compound **4** catalyzes the hydroformylation of terminal olefins with a faster rate. Furthermore, the selectivity of the formation of terminal aldehyde 1-heptanal is considerably high in the case of Al catalyst **2** (Table 1).

Scheme 2

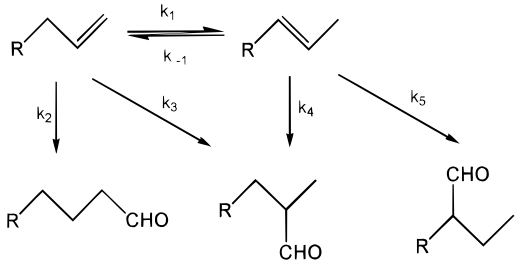

These observations put together can be explained by a simple reaction scheme involving the individual rate constants of the various processes as shown in Scheme 2. It appears from the data presented in Table 1 that the rate constants k_2 and k_3 are higher compared to k_1 in the case of Al and Ga catalysts **2** and **3**, while the reverse is true for In compound **4**.

In order to have a better understanding of the observed parameters listed in Table 1, we have performed additional experiments. The rate of formation of the various products in each case has been followed as a function of time by drawing small amounts of the catalytic mixture and analyzing them using a gas chromatograph. The results of these experiments for all three catalysts along with the observed n/iso ratio of the aldehydes are shown in Figure 7. In all the cases there is no observable induction period for the hydroformylation reactions to set in. This contrasts with the observation of the earlier workers with compounds $Co_3(CO)_9CR$ as the catalysts.[38] Another observation that is apparent in this figure is the rate of formation of the 2-hexene or internal olefins. The formation of these internal olefins in the case of Al catalyst **2** is very low and remains more or less constant as a function of time. In the case of **3**, the isomerization increases with time initially up to 2 h, indicating a considerable amount of isomerization. However, the ability of Ga catalyst **3** in hydroformylating the internal olefins decreases the amount of internal olefins present in the solution. In the case of In catalyst **4**, the rates of formation of both aldehydes and internal olefins increase as a function of time and the process is not complete even after 5 h. Also there is a drop in the n/iso ratio as a function of time in all the three cases (Table 1).

Since the effect of catalyst concentration on the catalytic process is likely to throw insight into the retention or decomposition of the catalytic structure,[39] we performed a series of catalyst concentration dependent hydroformylation runs. The results are pictorially represented in Figure 8. The turnover numbers quoted are those obtained after 3 h of the catalytic process.[40] It is evident from this figure that the increase in the concentration of catalysts **2** and **3** lowers the turnover numbers

(36) Feher, F. J.; Budzichowski, T. A. *J. Organomet. Chem.* **1989**, *379*, 33.

(37) Cornils, B. *Reactivity and structure concepts in organic chemistry 11: New synthesis with carbon monoxide*; Falbe, J., Ed.; Springer Verlag: Berlin, Heidelberg, New York, 1980.

(38) Withers, H. P.; Seyferth, D. *Inorg. Chem.* **1983**, *22*, 2931.

(39) Laine, R. M. *J. Mol. Catal.* **1982**, *14*, 137.

(40) A comparison of these values with that listed in Table 1 for catalytic runs carried out for 18 h indicates that the hydroformylation reaction is almost complete after 3 h in the case of **2** and **3**, while the reaction with **4** is only half-way through.

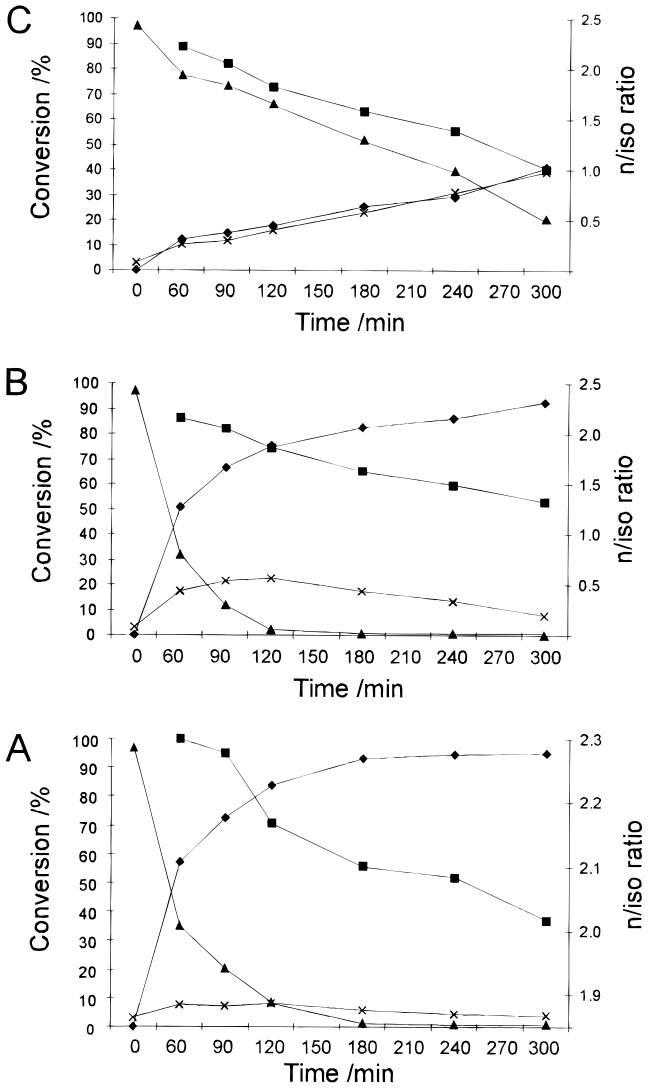

Figure 7. Product distribution and n/iso ratio of the aldehydes as a function of time in hydroformylation reaction of 1-hexene with **2** (A), **3** (B), and **4** (C) as catalysts (based on unrecovered 1-hexene): (■) n/iso ratio; (▲) 1-hexene; (◆) aldehydes; (×) 2-hexene (0.04 mmol catalyst, 120 °C, 70 bar, 160 mmol of 1-hexene charged; n/iso ratio represents the linear to branched aldehyde distribution).

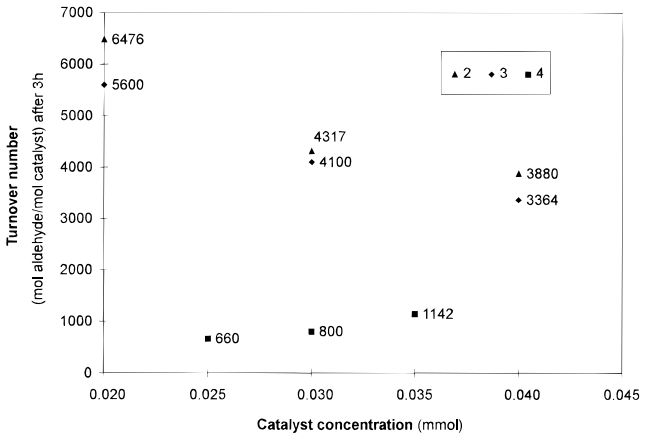

Figure 8. The effect of cluster concentration on aldehyde formation.

to a considerable extent. On the other hand, in the case of **4**, there is a slight increase in the observed turnover numbers. This observation is a possible indication that the catalytic process in the later case involving **4** is attributable to a cluster catalysis.[39] However, the decrease in the turnover number with concentration in the case of **2** and **3** does not necessarily mean that the cluster undergoes decomposition during the process. Additional studies discussed below however provide more convincing evidence for the cluster rearrangement in compound **4**.

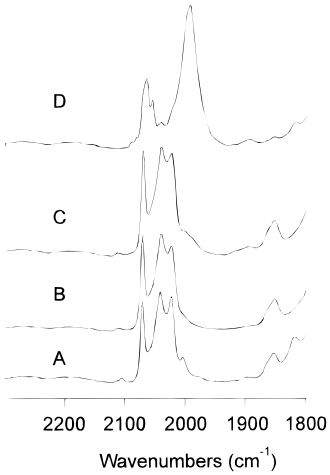

Figure 9. FTIR spectra of samples of $Co_2(CO)_8$ (A), **2** (B), **3** (C), and **4** (D) in catalytic hexane/hexene solution after 3 h at 120 °C and an initial pressure of 70 bar of H_2/CO (1:1).

We performed additional studies in solution using IR spectroscopy as the probe for examining the integrity of the $Co_3(CO)_9C$ cluster during the catalytic process. After 3 h of the catalytic process the spectra were recorded by drawing a small amount of the solution. The observed IR spectra in the CO region of all three mixtures along with the spectrum of a test run employing $Co_2(CO)_8$ as a catalyst are shown in Figure 9. It is instructive to compare the spectra displayed in this figure with those shown in Figure 1 in order to realize the changes effected by the catalytic process. Interestingly, the spectrum of $Co_2(CO)_8$ before and during catalysis remains almost the same while noticeable changes have taken place in the spectra of the heterosiloxane catalysts. As a representative case (galliumsiloxane **3**) the initially observed pattern containing two absorptions (at around 2040 and 2060 cm^{-1}) (Figure 1) changes into a three-line absorption pattern with the new peak appearing around 2020 cm^{-1} (Figure 9). The Al catalyst **2** also shows a very similar behavior. More strikingly, this pattern almost matches with the spectrum observed for $Co_2(CO)_8$ indicating the possibility of the $Co_3(CO)_9C$ cluster unit decomposing in solution into $Co_2(CO)_8$ during the process of catalysis.

In the case of the spectrum obtained using In catalyst **4**, such behavior is not observed. Instead there appears a new absorption at 1995 cm^{-1} (Figure 9). This spectrum does not have any common features with the spectrum obtained using $Co_2(CO)_8$ catalyst. This observation testifies to the fact that the catalytically active species in this case is not a $Co_2(CO)_8$ fragment although there exists some skeletal rearrangements of the basic $Co_3(CO)_9C$ unit of **4**. While these studies do not clearly reveal the type of the arrangement taking place in **4**, there are clear indications that the rearrangement during catalysis is a continuous process as evidenced by our time-dependent IR studies of this reaction mixture shown in Figure 10. For example, spectrum C recorded after 18 h is considerably different from spectrum B which was recorded only after 3 h.

In order to further verify the lability of CO ligands in these three heterosiloxane clusters, which will lead to the skeletal

(41) For the ^{13}C NMR measurements the $Co_3(CO)_9C$ units are enriched with ca. 20% ^{13}CO. The resonances of the apical carbon atoms could not be detected in the case of the Ga and In compounds **3** and **4** probably due to the line broadening owing to the spin−spin coupling with the three cobalt atoms.

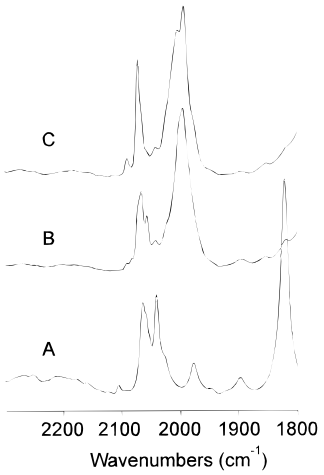

Figure 10. FTIR spectra of samples of **4** in catalytic hexane/hexene solution (initial charging pressure 70 bar of H_2/CO; 1:1): (A) 10 min at room temperature, (B) 3 h at 120 °C, (C) 18 h at 120 °C.

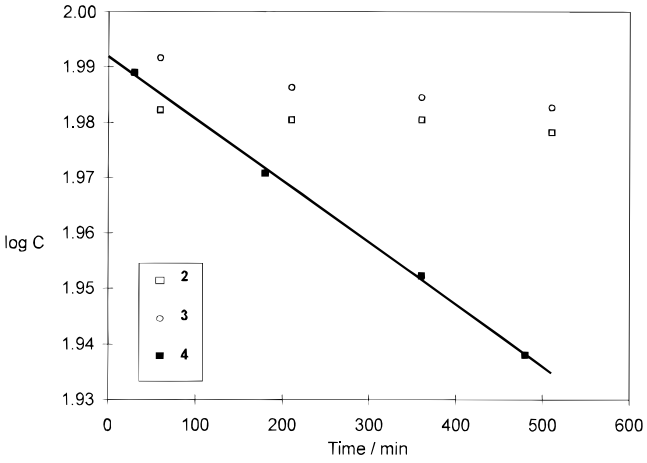

Figure 11. First-order rate plot for the disappearance of ^{13}CO from the gas phase over a toluene solution of the cluster at 22 °C. k_{obs} for compound **4** is 5.4×10^{-6} s^{-1}.

rearrangements of the cluster units, further experiments were performed with the aid of mass spectroscopy (eq 2). In a ^{13}CO

$$[Co_3(^{12}CO)_9CSiO_3E\cdot THF]_4 + n^{13}CO \rightleftarrows [Co_3(^{12}CO)_{9-n}(^{13}CO)_nCSiO_3E\cdot THF]_4 + n^{12}CO$$

filled Schlenk flask at 1 atm, 1 mL of the toluene solution containing 0.003 mmol of the heterosiloxane is introduced and stirred at constant temperature (22 °C) under identical conditions. From this flask a very small amount of the gas was drawn and analyzed in the mass spectrometer for the ^{12}CO/^{13}CO ratio. To avoid the ambiguity of the peak assignments, peak-matching high-resolution techniques were employed. The results of these studies shown in Figure 11 indicate that the ligand exchange is faster and facile in the case of In compound **4** than that observed for **2** and **3**. In fact these mass spectral data results are in accordance with the ^{13}CO NMR chemical shifts described *vide supra*. We also calculate from this experiment the first-order rate constant for the ^{12}CO/^{13}CO exchange process for In catalyst **4** to be 5.4×10^{-6} s^{-1}.

In summary, it appears from all of the studies described here that in the case of hydroformylation reactions catalyzed by the Al and Ga heterosiloxanes **2** and **3**, there is a decomposition of the cluster units into smaller fragments. The IR studies indicate that these smaller units presumably have structures close to that of $Co_2(CO)_8$. In the case of the In complex, there does not appear to be any major decomposition and the catalytic process mainly involves some continual skeletal rearrangements. The mass, IR, and ^{13}C NMR spectral studies lend evidence for this supposition.

Conclusion

In this paper, we have demonstrated the use of the cobalt carbonyl cluster anchored silanetriol **1** as the building block for the generation of novel group 13 heterosiloxane frameworks which are found to be soluble in common organic solvents such as THF. The molecular structure of the aluminosiloxane compound determined by X-ray crystallography shows the presence of three different types of $Co_3(CO)_9C$ cluster units within the same molecule. These heterosiloxanes have been demonstrated as useful catalysts under comparatively lower pressures in hydroformylation reactions involving terminal olefins, with a regioselectivity of over 60%. The solution studies on various catalytic mixtures indicate a possible decomposition of the heterosiloxane clusters **2** and **3** during the hydroformylation reactions. In view of these encouraging results, from what are essentially first generation group 13 heterosiloxane based molecular cobalt carbonyl clusters, one is inclined to believe that this synthetic route can prove useful for the design and generation of hydroformylation catalysts by appropriate modifications.

Experimental Section

General Data. All experimental manipulations were carried out under dry nitrogen atmosphere rigorously excluding air and moisture. The samples for spectral measurements were prepared in a drybox. Solvents were purified employing conventional procedures and were freshly distilled prior to use. NMR spectra were recorded on a Bruker AM 200 or a Bruker AS 400 instrument, and the chemical shifts are reported with reference to TMS. The upfield shifts are negative. IR spectra were recorded on a Bio-Rad Digilab FTS7 spectrometer (only the strong absorption bands are given *vide infra*). Mass spectra were obtained on a Finnigan MAT System 8230 and a Varian MAT CH5 mass spectrometer. Melting points were obtained on a HWS-SG 3000 apparatus, and compounds **2**−**4** do not melt below 200 °C. CHN analyses were performed by the Analytical Laboratory of the Institute of Inorganic Chemistry at Göttingen.

$Co_2(CO)_8$ (MERCK-Schuchard), 1-hexene (97%), heptane (spectroscopic grade), $AlMe_3$, $GaMe_3$, and ^{13}CO (99.7%) (all Aldrich), and $InMe_3$ (Strem) were used as received. $Co_3(CO)_9CSi(OH)_3$ was prepared using the procedure reported by Seyferth and co-workers.[23]

Catalysis Test. All hydroformylation reactions were carried out in a 300-mL stainless steel autoclave equipped with automatic temperature and stirring control. During the reaction process, samples were analyzed by gas chromatography and also GC-MS by comparing the retention time with those of authentic substances. The yields of the aldehydes were based upon the initial quantity of 1-hexene charged. These were determined by analytical GC (Varian 3700; column DB5, 30 m; carrier gas helium, 20 psi; split 1:100; FID detector) using heptane as an internal standard. Reactions were run with solutions of 30 mL of toluene and 20 mL of 1-hexene unless otherwise specified. The solutions containing the cluster and 1-hexene were pressurized at room temperature at 70 bar with a mixture of hydrogen-carbon monoxide (partial pressures: 1:1) and then heated to 120 °C.

Synthesis of $[Co_3(CO)_9CSiO_3Al\cdot THF]_4$ (2). In a two-necked round-bottomed flask (50 mL) equipped with a rubber stopper and bubble counter, **1** (0.52 g, 1.00 mmol) was dissolved in THF (14 mL). To this solution $AlMe_3$ (1.00 mmol, 2 mol/L of solution in hexane, 0.5 mL) in hexane (1 mL) was added dropwise during which spontaneous gas evolution was observed. The progress of the reaction was followed by means of pneumatic gas sampler. After 1 min, approximately 70 mL of methane had evolved indicating completion of the reaction. The reaction flask of one such run after adding hexane kept at −30 °C for a period of 3 months produced deep-violet square-shaped crystals suitable for X-ray crystal structure analysis. A total yield of the

crystalline compound **2** was found to be 0.27 g (0.11 mmol, 43%). Elemental analysis Calcd for $C_{56}H_{32}Al_4Co_{12}O_{56}Si_4$ (2464.3): C, 27.5; H, 1.3; Si, 5.4. Found: C, 25.5; H, 2.4; Si, 6.1 (the smaller C content is due to cobalt carbide formation). ^{13}C NMR (100.6 MHz, THF-d_8, TMS) 25 °C: δ 199.4 (s, CO); 203.2 (s, CO); 262.2 (s, μ^3-C). ^{29}Si NMR (79 MHz, C_6D_6, TMS): δ −73.6. IR (KBr, Nujol): $\tilde{\nu}$ 2055 (ss); 1969 (w).

Syntheses of $[Co_3(CO)_9CSiO_3E\cdot THF]_4$ (E = Ga (3), In (4)). In a two-necked round-bottomed flask (50 mL) equipped with a reflux condenser and bubble counter, **1** (0.52 g, 1.00 mmol) was dissolved in THF (14 mL) and heated to 60 °C. EMe_3 (1 mmol, $GaMe_3$ 3 mol/L of solution in *n*-hexane, $InMe_3$ dissolved in 10 mL of THF) was added dropwise and the solution was heated for an additional 2 h. The solvent was distilled *in vacuo* and the product could be isolated quantitatively in the form of a black violet powder. Further purification was achieved by cooling a THF/hexane solution of the respective compounds.

$[Co_3(CO)_9CSiO_3Ga\cdot THF]_4$ (3). Yield 0.63 g (93%). Mp 205 °C dec. Elemental analysis Calcd for $C_{56}H_{32}Co_{12}Ga_4O_{56}Si_4$ (2699.24): C, 24.9; H, 1.2. Found: C, 23.5; H, 1.5. MS (EI, *m*/*z* (%)): 217 (5, Co_3CSi), 59 (100, Co). IR (CsI, Nujol): $\tilde{\nu}$ 2106 (w); 2062 (ss); 2038 (s). ^{1}H NMR (200 MHz, C_6D_6): δ 1.25 (m, THF), 3.48 (m, THF). ^{13}C NMR[41] (62.9 MHz, THF-d_8) 25 °C: δ 200.6, 202.2, 209.3 (CO). ^{13}C NMR[41] (62.9 MHz, THF-d_8) −90 °C: δ 201.1, 204.9, 214.8 (CO). ^{29}Si NMR (49.7 MHz, THF/C_6D_6): δ −63.6.

$[Co_3(CO)_9CSiO_3In\cdot THF]_4$ (4). Yield 0.66 g (91%). Mp 215 °C dec. Elemental analysis Calcd for $C_{56}H_{32}Co_{12}In_4O_{56}Si_4$ (2879.63): C, 23.0; H, 1.1. Found: C, 22.1; H, 1.6. MS (EI, *m*/*z* (%)): 217 (100, Co_3CSi). IR (CsI, Nujol): $\tilde{\nu}$ 2105 (w); 2059 (ss); 2037 (ss). ^{1}H NMR (200 MHz, C_6D_6): δ 1.23 (m, THF), 3.44 (m, THF). ^{13}C NMR[41] (62.9 MHz, THF-d_8) 25 °C: δ 200.2, 202.0 (CO). ^{13}C NMR[41] (62.9 MHz, THF-d_8) −90 °C: δ 200.6, 202.6 (CO). ^{29}Si NMR (49.7 MHz, THF/C_6D_6): δ −62.5.

Crystal Structure Determination. Data for **2**: $[Co_3(CO)_9CSiO_3Al\cdot THF]_4$ + THF + hexane, M = 2577.47, monoclinic, space group $P2_1/c$, a = 1320.6(3) pm, b = 3289.4(7) pm, c = 2262.0(5) pm, β = 104.77(3)°, V = 9.501(4) nm^{-3}, Z = 4, ρ_{ber} 1.802 Mg m^{-3}, *F(000)* = 5124, λ = 71.073 pm, T = 153(2) °C, μ(Mo Kα) = 2.220 mm^{-1}, crystal size 0.8 × 0.5 × 0.5 mm, 4° < 2θ < 45°, 12661 total reflections, 12402 independent, refinements of 1379 parameters, semiempirical absorption correction using ψ-scans; large electron density residue: 744 e nm^{-3}, R_1(for $F>4\sigma(F)$) = 0.061 and wR_2 = 0.168 (all data) with $R_1 = \sum||F_o| - |F_c||/\sum|F_o|$ and $wR_2 = (\sum w(F_o^2 - F_c^2)^2/\sum w(F_o^2)^2)^{0.5}$.

The data were collected on a Stoe-Huber diffractometer. The measurements of the intensities were determined with a cooled crystal in an oil drop according to the 2θ/ω-range.[28] The structure was solved by direct methods (SHELXS-90)[29] and refined using the least-squares method on F^2.[30] The disordered $Co_3(CO)_9C$ was refined on two positions with occupation factors of 0.49/0.51 with the aid of restraints. In the single uncoordinated THF molecule in the asymmetric unit, the position of the oxygen atom could not be localized. The hexane molecule in the lattice was refined using 1−2 and 1−3 restraints.

Acknowledgment. This work was supported by the Fonds der Chemischen Industrie, the Deutsche Forschungsgemeinschaft, and the Hoechst AG. U.R. thanks the Fonds der Chemischen Industrie for a Liebig Fellowship. R.M. thanks the Alexander von Humboldt Foundation for a Research Fellowship.

Supporting Information Available: Tables of atomic coordinates and anisotropic parameters of all atoms, bond distances, and angles of **2** (19 pages). See any current masthead page for ordering and Internet instructions.

JA952986W